

Full factorial design to assess the concrete gas permeability

C. Argiz¹ and M.A. Sanjuán^{2,*}

¹Civil Engineering School, Polytechnic University of Madrid, C/ Profesor Aranguren, s/n, Ciudad Universitaria, 28040 Madrid, Spain; ²Spanish Institute of Cement and its Applications (IECA), C/ José Abascal, 53, 28003 Madrid, Spain.

Diseño factorial de experimentos completo para la evaluación de la permeabilidad a los gases del hormigón

Disseny factorial d'experiments complet per l'avaluació de la permeabilitat als gasos del formigó

RECEIVED: 16 DECEMBER 2016; ACCEPTED: 9 JANUARY 2017

SUMMARY

Novel composite material durability is mainly affected by the transport of fluids and ions through the pore system which are potentially able to produce damage. Then, a key indicator of long-term durability of the structures can be the ease with which aggressive agents are transported through the pore system, i.e. composite material permeability. The purpose of this paper is to broaden our knowledge of air permeability testing conditions and, in particular, how it is affected by the preconditioning temperature and testing pressure. Optimization of variables to determinate the air permeability coefficient was done by using a 2³ full factorial design. Air permeability results are recorded in Ø150x70 mm³ concrete specimens. The air permeability determination procedure gives reliable information about the quality of concrete with regard to its durability.

Keywords: Concrete; durability; full factorial design; Non-destructive testing.

RESUMEN

La durabilidad de los nuevos materiales compuestos viene influenciada, principalmente, por el transporte de fluidos y de iones a través del sistema de la red de poros, los cuales son potencialmente capaces de producir daños. Por tanto, un indicador clave para establecer la durabilidad de las estructuras a largo plazo puede ser la facilidad con la que los agentes agresivos son transportados a través del sistema de poros, es decir, la permeabilidad del material compuesto.

El objeto de este artículo es la ampliación de nuestro conocimiento sobre las condiciones de ensayo de la permeabilidad al aire y, en particular, cómo la temperatura de pre-acondicionamiento y la presión de

ensayo influyen en él. La optimización de las variables para obtener el coeficiente de permeabilidad al aire se realizó con un diseño factorial de experimentos completo 2³. Los resultados de permeabilidad al aire se obtuvieron en probetas de hormigón cilíndricas de dimensiones Ø150x70 mm³. El procedimiento de la determinación de la permeabilidad al aire da una información fiable de la calidad del hormigón con relación a su durabilidad.

Palabras clave: Hormigón; durabilidad; diseño factorial completo; ensayos no destructivos.

RESUM

La durabilitat dels nous materials compostos ve influenciada, principalment, pel transport de fluids i de ions a través del sistema de la xarxa de porus, els quals són potencialment capaços de produir danys. Per tant, un indicador clau per establir la durabilitat de les estructures a llarg termini pot ser la facilitat amb què els agents agressius són transportats a través del sistema de porus, és a dir, la permeabilitat del material compost.

L'objecte d'aquest article és l'ampliació del nostre coneixement sobre les condicions d'assaig de la permeabilitat a l'aire i, en particular, com la temperatura de pre-condicionament i la pressió d'assaig hi influeixen. L'optimització de les variables per obtenir el coeficient de permeabilitat a l'aire es va realitzar amb un disseny factorial d'experiments complet 2³. Els resultats de permeabilitat a l'aire es van obtenir en provetes de formigó cilíndriques de dimensions Ø150x70 mm³. El procediment de la determinació de la permeabilitat

*Corresponding author: masanjuan@ieca.es

a l'aire dóna una informació fiable de la qualitat del formigó amb relació a la seva durabilitat.

Paraules clau: Formigó; durabilitat; disseny factorial complet; assajos no destructius.

INTRODUCTION

Currently, a performance criterion to get a reliable durability estimation of new composite materials based on concrete is one of the main topics regarding the concrete research field¹. Several years ago, compressive strength was considered as the only indicator for concrete durability. Recently, durability control was guaranty by fixing lower limits of compressive strength, cover thickness and curing time. Also, upper limits of some constituents and mix proportions (water-cement ratio) were established². Nevertheless, the durability of the new concrete composite materials is governed mainly by resistance to be penetrated by aggressive agents¹. Such resistance is related to the moisture degree and pore structure of the composite. As a consequence, permeability can be estimated by means of the air permeability coefficient which might be taken as a reliable estimator of durability. Gas permeability stands as a critical material parameter, which characterizes the structure and the durability of novel composite materials³.

The air permeability coefficient is not only influenced by the quality of the material, but also by the preconditioning of the sample before testing. Then, it is essential to establish the preconditioning and testing conditions in order to get a good relationship between permeability and durability.

Permeability and porosity relationship in hardened cement paste is well-known⁴⁻⁷. Porosity sizes ranges from 30 to 40 percent by volume in hardened cement paste⁸ with either gel or capillary pores which have diameters about 2 nm and 1000 nm, respectively. Particularly, pores greater than 132 nm have a strong influence on cement paste permeability⁷ as well as their shape and interconnection. Permeability of concrete can be about 100 times greater than cement paste permeability⁸. The reason of this huge difference can be found in the effect of the aggregates and the cement paste-aggregate transition zone on the material. Novel composites exhibit much lower permeability is required for especial applications⁹. Concrete gas permeability testing methods have been developed to check the quality of the concrete. In all the cases is of great importance the sample preconditioning^{10,11,12} and testing conditions¹³ to reach a good testing reproducibility¹⁴.

Some fluids have been proposed to measure permeability of cement-based composites: water, solutions, oil, air, oxygen, nitrogen, water vapor, and so on¹⁵⁻¹⁶. Aqueous solutions have as a disadvantage the potential reaction with the cement phases modifying the real permeability. On the other hand, gas permeability testing methods depend on the sample moisture content, and therefore, testing samples must be preconditioned usually by drying the specimen. The way

in which preconditioning process is performed has a direct effect on the outcome of tests¹⁷.

Microcracking will form in the cement matrix in reinforced concrete induced by drying when the structures are kept in an environment not immersed in water. Also, microcracks can be formed by the action of external forces and heating gradients¹⁸. Thus, civil engineers need to get a preliminary knowledge about how novel composite materials used in structures will behave under real conditions, i.e. its ability to crack. The aim of this study is to investigate the best use of a preconditioning temperature and testing pressure taken into account the water-cement ratio of the concrete. In this study, the experimental system was modeled using a 2³ full factorial experimental design¹⁹.

EXPERIMENTAL SECTION

Materials and testing specimens

A common Portland cement CEM I 32.5 N according to the European standard EN 197-1:2011²⁰ and siliceous aggregates with a maximum size of 30 mm were used.

Cylindrical concrete specimens of Ø15 x 30 cm with two water/cement ratios of 0.42 and 0.52 were made. Table 1 shows the concrete dosage. The casting was done in two layers and the mass was consolidated by vibration. Then, the specimens were cured at 100% of relative humidity for 24 hours. Later, the specimens were kept at 25°C or oven-dried at 40°C up to a constant weight before testing. Cylindrical concrete specimens were cut into Ø15 x 7 cm discs. The 28-day compressive strength was 30 MPa tested in Ø15 x 30 cm cylindrical specimens.

Table 1. Concrete mixes (kg per cubic meter).

Concrete	A	B
Water/cement	0.42	0.52
Gravel	372	372
Pebble	842	842
Sand	628	628
Cement	382	307
Water	160	160

Testing procedure

Gas permeability testing was performed following the RILEM recommendations²¹. Concrete air permeability experimental testing system is shown in Fig. 1, which is composed of two metallic cells placed at each side of the concrete specimen. Both of them were designed to stand for pressure of 50 MPa. In the first one, inlet air is held at the chosen pressure by means of a compressor controlled by a precision pressure regulator. In the second one, the passing air is collected in a cylinder and the outflow is measured at atmospheric pressure. The air flow rate is measured in steady-state conditions. The two cells were screwed to the concrete specimens leaving a circular passing area of 0.005 m² in both sides.

Air flow, Q (m³.s⁻¹), at the environmental temperature, T , and pressure, P , under steady-state conditions was recorded. It was then transformed to normal conditions by using equation (1), where Q_0 , P_0 and T_0 are

the air flow, pressure and temperature at normal conditions, respectively. This transformation leads to remove the air kinematic viscosity increase and air volume expansion effects when the temperature increases.

$$Q_0 = \frac{T_0 P}{T P_0} \cdot Q \quad (1)$$

The Hagen-Poiseuille equation was used to determine the air permeability coefficient, D_{air} (m^2) in steady-state conditions (equation (2)). This equation can be used for a compressible fluid with laminar flow passing through a porous material composed of a network of small capillary pores from air flow data, Q ($m^3 \cdot s^{-1}$).

$$D_{air} = 2L\eta \frac{Q}{A(P^2 - P_a^2)} \quad (2)$$

Air dynamic viscosity, η , is $1.8 \cdot 10^{-5}$ N.s. m^{-2} at $20^\circ C$. The absolute inlet pressures in the test method, P , have been 200 mmHg (26,665 N m^{-2}) and 400 mmHg (53,329 N m^{-2}); whereas the outlet and measuring pressures, P_a and P_o , respectively, were equal to the atmospheric pressure. The specimen cross-sectional area, A , was 0.005 m^2 and the thickness, L , was 0.07 m.

Taking into account the inlet, outlet and measuring pressures, P , P_a and P_o , respectively, the specimen thickness, L , and the cross-sectional area, A in equation (2), the air permeability coefficient can be calculated for each pressure directly from the air flow data, Q ($m^3 \cdot s^{-1}$), by means of equations (3) and (4).

$$D_{air(200mmHg)} = 5.34 \cdot 10^{-9} Q_{200mmHg} [m^2] \quad (3)$$

$$D_{air(400mmHg)} = 6.88 \cdot 10^{-9} Q_{400mmHg} [m^2] \quad (4)$$

Determination of the experimental error

In order to calculate the experimental error of the gas permeability method, the ideal gas equation shown in equation (5) was differentiated, and then, the finite increments equation (6) was obtained.

$$\frac{P \times V}{T} = n \times R = \text{CONSTANT} \quad (5)$$

$$\frac{\Delta V}{V} = \frac{\Delta T}{T} - \frac{\Delta P}{P} \quad (6)$$

Considering the testing air permeability conditions, a volume of 0.01 m^3 , a pressure of 710 mmHg and a temperature of 293 K, were used.

To calculate the error (ϵ) of non-considering the pressure and temperature variations, values of temperature and pressure of $1^\circ C$ and 1 Torr were taken as shown in equation (7).

$$\epsilon = 100 \times \frac{\Delta V}{V} = \left(\frac{1}{293} \pm \frac{1}{710} \right) \times 100 = 0.2\% - 0.5\% \quad (7)$$

The experimental error, ϵ , ranges from 0.2% to 0.5%. For testing volumes between 50 and 500 cm^3 , pressure and temperature variations of one unit leads to an error equal to the same order of magnitude than the measured value (equation (8)).

$$\frac{\Delta V}{V} \times 100 = 0.5\% - 5\% \quad (8)$$

Given that, non-corrected pressure and temperature values provide an error range from 0.5% to 5% of vol-

ume. Summing up, parameter correction is of great importance.

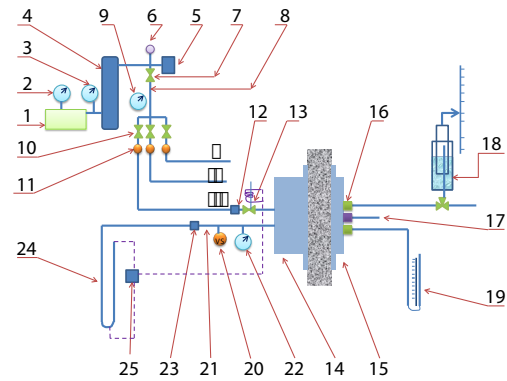


Figure 1. Air permeability testing system: (1) Compressor with a maximum pressure of 7355 mmHg; (2) and (3) Stainless steel manometers of 5884 mmHg; (4) Compressed air reservoir; (5) Pressure gauge "Billman" PD38 type (ΔP from 3 to 8 kg/cm^2); (6) Safety valve set at 4 kg/cm^2 ; (7) 1/2" in-take valve; (8) relief valve; (9) Iron manometer of 5 Kg/cm^2 ; (10) 1/2" in-take valves; (11) 3/8" SAE connecting nuts; (12) 1/2" SAE connecting nut; (13) Solenoid check valve "DANFOSS" EVJ 10 - 220V type; (14) inlet pressurized air cell; (15) outlet air cell; (16) 3/8" SAE connecting nut; (17) Mercury thermometer; (18) Cylinder containing a piston which collects the outflow (12 cm diameter and 50 cm height); (19) Manometer U-type; (20) Safety valve (set at 2.5 Kg/cm^2); (21) relief valve; (22) Metallic manometer of 3 Kg/cm^2 ; (23) 3/8" SAE connecting nuts; (24) Manometer U-type; (25) Inlet air pressure electrical control system. Units: 1mmHg (1 Torr) = 133.32236 N. m^{-2} (Pa)

RESULTS AND DISCUSSION

Modeling approach

In order to compare the experimental results with the theoretical calculations and optimize the testing conditions, a full factorial design was used. In this method, once the experimental design was determined and the trials were carried out, the measured performance characteristic from each trial was used to analyze the relative effect of the different parameters. Then, the factorial design is used to evaluate three factors simultaneously. The treatments are combinations of levels for each factor. The advantages of factorial designs over one factor at a time experiments are that they are more efficient and, also, they allow interactions to be detected¹⁹.

Full factorial experimental design

A design structure was determined which is called full factorial design. In this design, three factors and two levels were chosen (2^3 design). Then, it requires a total of 8 experiments which is found adequate to determine the effects of water/cement (w/c), pre-conditioning temperature and testing pressure on air permeability coefficient, D_{air} . The selected levels were 0.42 and 0.52 for w/c, 25 and $40^\circ C$ for pre-conditioning temperature and, finally, 200 and 400 mmHg for

testing pressure. The experimental set up is given in Table 2. The resulting outcome is the air permeability coefficient of the concrete, D_{air} . The complete design matrix together with the response values obtained from the experimental work is given in Table 2.

Table 2. Experimental setup.

Run	Experimental Point	Experimental Matrix			Experimental Plan			Response
		x1	x2	x3	Pressure (mmHg)	Temperature (°C)	water/cement	
								D_{air} ($\times 10^{-16} m^2$)
1	y1	-	-	-	200	25	0.42	9.228
2	y2	+	-	-	400	25	0.42	9.032
3	y3	-	+	-	200	40	0.42	12.82
4	y4	+	+	-	400	40	0.42	12.64
5	y5	-	-	+	200	25	0.52	16.01
6	y6	+	-	+	400	25	0.52	15.55
7	y7	-	+	+	200	40	0.52	19.61
8	y8	+	+	+	400	40	0.52	19.44
							Grand Mean	14.29

Summarizing up, a total of 8 tests were performed to obtain the effects of w/c, pre-conditioning temperature and testing pressure on air permeability coefficient, D_{air} . The materials designer can control these three variables during the testing process (each at two levels):

- Factor A: Pressure with levels 200 and 400 mmHg.
- Factor B: Preconditioning temperature with levels 25 and 40°C.
- Factor C: Water-cement ratio with levels 0.42 and 0.52.
- Unit: D_{air} .
- Response variable: Deviation from the actual D_{air} .

Thus, six hypotheses will be simultaneously tested. In Table 2, minus symbol (-) represents factors A, B and C at the low level whereas plus symbol (+) represents factors A, B and C at the high level. The minimum value of air permeability coefficient recorded was $9.032 \times 10^{-16} m^2$, this value corresponds to 0.42, 25°C and 400 mmHg testing parameters; whereas the maximum one was $19.61 \times 10^{-16} m^2$ and this value corresponds to 0.52, 40°C and 200 mmHg testing parameters. According to the experimental data, air permeability coefficient, D_{air} , increases by oven-drying the concrete specimens up to 40°C ($D_{air} = 19.61 \times 10^{-16} m^2$). On the contrary, the value of air permeability coefficient, D_{air} , decreases when the pressure of gas injection increases due to the slip phenomenon²².

While the overall average of the results (i.e. the Grand Mean) is 14.29×10^{-16} , the average of the results for A- (factor A run at low level) is $((9.228+12.82+16.01+19.61) \times 10^{-16}) / 4 = 1.44154 \times 10^{-15}$; whereas 1.41635×10^{-15} is the average value of the test results for A+ (factor A run at a high level). The B and C averages at low and high levels are also calculated (Table 3).

A main effect is the difference between the factor average and the Grand Mean (Table 3). These main effects or effect sizes determine which factors have the most significant impact on the results. Finally, Table 3 also shows the sum of squares (SS). Then, calculations in ANOVA determine the significance of each factor based on these effect calculations.

Table 3. A, B and C averages, main effects and main effects squared at low and high levels (D_{air} , m^2) and sum of squares (SS).

	A avg.	B avg.	C avg.	A Effect	B Effect	C Effect	A effect squared	B effect squared	C effect squared
low	1.44×10^{-15}	1.25×10^{-15}	1.09×10^{-15}	1.26×10^{-17}	-1.84×10^{-16}	-3.36×10^{-16}	1.59×10^{-34}	3.37×10^{-32}	1.13×10^{-31}
high	1.42×10^{-15}	1.61×10^{-15}	1.77×10^{-15}	-1.26×10^{-17}	1.84×10^{-16}	3.36×10^{-16}	1.59×10^{-34}	3.37×10^{-32}	1.13×10^{-31}
Sum of Squares (SS)				SS_A		SS_B		SS_C	
SS				1.2692×10^{-33}		2.69527×10^{-31}		9.04×10^{-31}	

Main Effects are a quick and efficient way to visualize effect size. Fig.2 shows that C+ has a higher mean D_{air} than C-. B+ also has a higher mean value than B-. On the contrary, A- has a higher mean D_{air} than A+. In addition, the size effect of factor C, water-cement ratio, is larger than the other two factor effects.

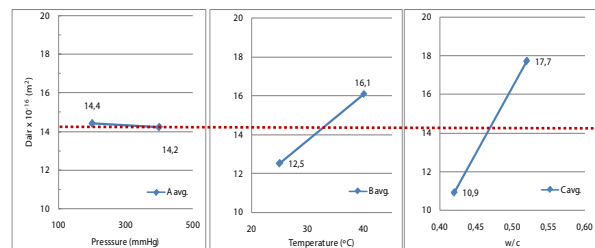


Figure 2. Main effects for results ($D_{air} \times 10^{-16} m^2$).

Interaction Effects

With the aim of determining the main effects for each factor, it is often significant to identify how multiple factors interact in effecting the results. An interaction occurs when one factor effects the results differently depending on a second factor. For instance, to find the AB interaction effect, first, the average result for each of the four level combinations of A and B was calculated. Given that, the average value when factors A and B are both at the low level, $(9.228 \times 10^{-16} + 16.01 \times 10^{-16}) / 2 = 12.62 \times 10^{-16}$, was calculated. And then, the mean when factors A and B are both at the high level, $(12.64 \times 10^{-16} + 19.44 \times 10^{-16}) / 2 = 16.04 \times 10^{-16}$, was also calculated. Following the same procedure, the average result for each of the remaining levels, AC and BC, was also calculated. Then, in this work, there are 8 runs (observations) and 8 ABC interaction levels (Tables 4 and 5).

Fig. 3 shows the interaction (or 2-way effects) of all three factors. When the lines are parallel, interaction effects are null. The more different the slopes, the more influence the interaction effect has on the results. To visualize these effects, the Y axis is always the same for each combination of factors. According to Fig. 3, the BC interaction effect is the largest (Temperature and water-cement ratio).

The size effect is the difference between the average and the partial fit; whereas the partial fit is the effect of all the influencing factors. For main effects, the partial fit is the Grand Mean. For instance, the effect of AB is calculated according to equation (9).

Effect of AB = ABAvg.--[effect of A + effect of B + the Grand Mean] (9)

The effect size for 3-way interactions is calculated by finding the appropriate average and subtracting the partial fit. Then, to calculate the ABC effect when A and B are high and C is low (A+B+C-), equation (10) is applied.

Effect of (A+B+C-) = A+B+C-average -[A+effect + B+effect + C-effect + A+B+effect + A+C-effect + B+C-effect + Grand Mean] (10)

It is quite convenient to notice that each effect column sums to zero (Table 3). This will always be true whenever calculating effects. This is not surprising since effects measure the unit deviation from the observed value and the mean.

Table 4. Interaction effects setup.

Run	Effect Matrix							
	Average	x1	x2	x3	x1*x2	x1*x3	x2*x3	x1*x2*x3
1	+	-	-	-	+	+	+	-
2	+	+	-	-	-	-	+	+
3	+	-	+	-	-	+	-	+
4	+	+	+	-	+	-	-	-
5	+	-	-	+	+	-	-	+
6	+	+	-	+	-	+	-	-
7	+	-	+	+	-	-	+	-
8	+	+	+	+	+	+	+	+

Table 5. Interaction effects results.

Parameter	Interaction effects	D _{air} (x 10 ⁻¹⁶ m ²)
0 (Average)	(+ y1 + y2 + y3 + y4 + y5 + y6 + y7 + y8) / 8	14.2895
A	(- y1 + y2 - y3 + y4 - y5 + y6 - y7 + y8) / 4	-0.251908
B	(- y1 - y2 + y3 + y4 - y5 - y6 + y7 + y8) / 4	3.67101
C	(- y1 - y2 - y3 - y4 + y5 + y6 + y7 + y8) / 4	6.7214
AxB	(+ y1 - y2 - y3 + y4 + y5 - y6 - y7 + y8) / 4	0.0736998
AxC	(+ y1 - y2 + y3 - y4 - y5 + y6 - y7 + y8) / 4	-0.0620141
BxC	(+ y1 + y2 - y3 - y4 - y5 - y6 + y7 + y8) / 4	0.0735081
AxBxC	(- y1 + y2 + y3 - y4 + y5 - y6 - y7 + y8) / 4	0.0680099
Parameter	Interaction effects	D _{air} (x 10 ⁻¹⁶ m ²)

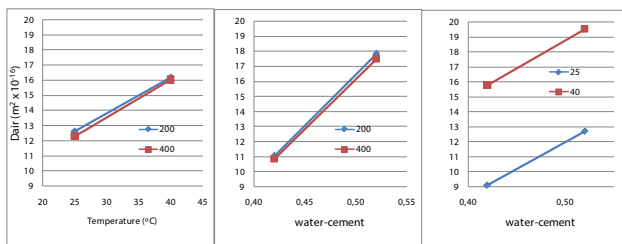


Figure 3. Interaction plots for results ($D_{air} \times 10^{-16} m^2$).

Analysis of variance (ANOVA)

Although effect plots help to visualize the impact of each factor combination, and also, they are quite useful to identify which factors are most influential, a statistical hypotheses test is needed in order to determine if any of these effects are significant. ANOVA is a statistical technique that subdivides the total variation, in a set of data, into element items relating to specific sources of variation for the purpose of testing hypotheses on the parameters of the model. Therefore, the statistical significance of the ratio of mean square variation due to regression and mean square residual error was checked using ANOVA method²³.

Analysis of variance (ANOVA) consists of simultaneous hypothesis tests to determine if any of the effects are significant (Table 6). When “factor effects are zero” this means that “the means for all levels of a factor are equal”. Thus, for each factor combination ANOVA tests the null hypothesis that the population means of each level are equal, versus them not all being equal. Several calculations have been made for each main factor and interaction term as shown in Table 6. Results in Table 6 show that there are only two significant parameters: Temperature and water/cement ratio. These results support that the concrete permeability is determined not only by concrete dosage, but also by the percentage and distribution of macro-pores.

Table 6. Analysis of variance (ANOVA).

SOURCE	DF	SS	MS	F	p-value	F-critical value	Remark
A	1	1.27E-33	1.27E-33	13.72	0.105	161	No significant
B	1	2.70E-31	2.70E-31	2913.59	0.139	161	Significant
C	1	9.04E-31	9.04E-31	9767.33	0.177	161	Significant
A x B	1	1.09E-34	1.09E-34	1.17	0.374	161	No significant
A x C	1	7.69E-35	7.69E-35	0.83	0.705	161	No significant
B x C	1	1.08E-34	1.08E-34	1.17	0.500	161	No significant
Error	1	9.25E-35	9.25E-35				

Sum of Squares (SS)= sum of all the squared effects for each factor, Degrees of Freedom (df)= number of free units of information, Mean Square (MS)= SS/df for each factor, Mean Square Error (MSE), Mean Square Error (MSE)= pooled variance of samples within each level, FF-statistic = MS for each factor/MSE.

Modeling approach

A polynomial regression equation was obtained by using a central composite design to analyze the factor interactions by identifying the significant factors contributing to the regression model. The ANOVA for the fitted equation shown in Table 7 shows the performance of the full factorial design. The ANOVA results showed that the equations adequately represented the real relationship between the significant variables and response. This design is generally used for fitting the second order model by the regression method as shown in equation (11).

$$D_{air} (x 10^{-16} m^2) = \beta_0 + \sum_{i=1}^n \beta_i x_i + \left(\sum_{i=1}^n \beta_i x_i \right)^2 + \left(\sum_{i=1}^{n-1} \sum_{j=i+1}^n \beta_{ij} x_i x_j \right) \quad (11)$$

where β_0 is the constant term, β_1 is the slope or linear effect of the input factor x_i , β_{ij} is the linear by linear interaction effect between the input factor x_i and x_j .

The final empirical model in terms of coded factors after excluding the insignificant terms for testing pressure is shown in equation (12) and Fig. 4.

$$D_{air} (x 10^{-16} m^2) = -4.986 + 48.406 T - 0.786 WC + 16.678 T^2 + 0.015 WC^2 + 0.097 T*WC \quad (12)$$

Generally, adjusted R² value is used for the accuracy of the modeled system. In this case, adjusted R² is

calculated as 0.9907 and it means that the accuracy of the equation (12) is 99.07%. This model provides reasonable predictions as some concrete air permeability models generated elsewhere¹.

Positive sign in front of the terms indicates synergistic effect, whereas negative sign indicates antagonistic effect. The quality of the model developed was evaluated based on the correlation coefficient value. The R^2 value for equation (12) was 0.9987. This indicated that 99.87% of the total variation in the D_{air} was attributed to the experimental variables studied. The closer the R^2 value to unity, the better the model will be as it will give predicted values which are closer to the actual values for the response. The R^2 of 0.9987 for equation (12) is considered relatively high, indicating that there was a good agreement between the experimental and the predicted D_{air} .

Analysis of variance (ANOVA) was further carried out to justify the adequacy of the model. The ANOVA for the quadratic model for D_{air} is listed in Table 7. From the ANOVA for response surface quadratic model for D_{air} , the Model F-value of 301.61 and Prob > F of 0.0033 implied that the model was significant.

Table 7. Analysis of variance (ANOVA).

Source	Sum of Squares	DF	Mean Square	F Statistic	P>F
Regression	117.36904	5	23.473808	301.607	0.00331
Error	0.155658	2	0.077829		
Total	117.5247	7			

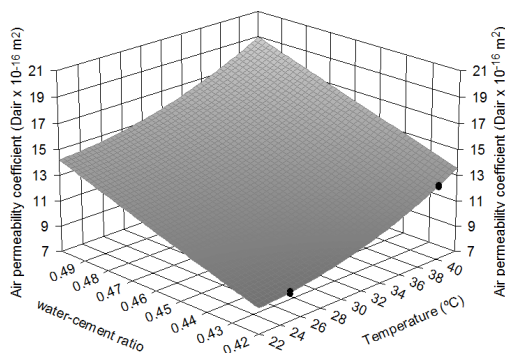


Figure 4. Three-dimensional response surface plot of air permeability coefficient ($D_{air} \times 10^{-16} m^2$) (effect of preconditioning temperature and water-cement ratio).

CONCLUSIONS

A quadratic model was developed to correlate the significant variables to the D_{air} . Interaction between the most important preconditioning parameter (temperature), testing variable (pressure) and concrete characteristic (water-cement ratio) with regard to the air permeability coefficient (D_{air}) have been evaluated. The main conclusions are summarized as follow:

- Testing pressure is not a significant variable.
- Preconditioning temperature and concrete quality (water-cement ratio) were found to have the greatest effect on concrete air permeability coefficient (D_{air}).

- Analyzing the measured responses, the fit summary of the output indicates that the model is statistically highly significant on the air permeability coefficient (D_{air}).
- Air permeability test is a reliable method to assess the concrete quality.

ACKNOWLEDGMENTS

Authors gratefully acknowledge to Prof. Rafael Muñoz-Martialay for his support and valuable advice in the experimental phase of this study. The authors also wish to thank to the Nuclear Applications Committee for the Public Works from Spain for their kind cooperation with this work.

REFERENCES

1. Balcikanli, M.; Ozbay, E. Optimum design of alkali activated slag concretes for the low oxygen/chloride ion permeability and thermal conductivity. *Composites Part B*. **2016**, *91*, 243-256.
2. EN 206-2016. Concrete Performance Production, Placing and Compliance Criteria; CEN, the European Committee for Standardization, Brussels, Belgium, 2016.
3. Bubacz, M.; Beyle, A.; Hui, D.; Ibeh, C.C. Helium permeability of coated aramid papers. *Composites Part B*. **2008**, *39*, 50–56.
4. Schönlin, K.; Hilsdorf, H.K. Permeability as a measure of potential durability of concrete -development of a suitable test apparatus. In: Proceedings of ACI SP-108-06: Permeability of concrete. Detroit, Michigan, USA, 1988, 99-115.
5. Powers, T.C.; Copeland, L.E.; Hayes, J.C.; Mann, H.M. Permeability of Portland cement paste. *Proc J Am Concr Inst*. **1954**, *51*, 285-298.
6. Goto, S.; Roy, D.M. The effect of w/c ratio and curing temperature on the permeability of hardened cement paste. *Cem Concr Res*. **1981**, *11*, 575-579.
7. Nyame, B.K.; Illson, J.M. Relationships between permeability and pore structure of hardened cement paste. *Mag Concr Res*. **1981**, *33*, 139-146.
8. Young, F.J. Review of the pore structure of cement paste and concrete and its influence on permeability, permeability of concrete. In: Proceedings of ACI SP-108-06: Permeability of concrete. Detroit, Michigan, USA, 1988, 1-18.
9. Sukjoo, C.; Sankar, B.V. Gas permeability of various graphite/epoxy composite laminates for cryogenic storage systems. *Composites: Part B*. **2008**, *39*, 782–791.
10. Ewertson, C.; Peterson, P.E. The influence of Curing Conditions on the permeability and durability of concrete. Results from a field exposure test. *Cem Concr Res*. **1993**, *23*, 683-692.
11. Kumar, A.; Roy, D.M. The effect of desiccation on the porosity and pore structure of freeze dried hardened portland cement and slag-blended pastes. *Cem Concr Res*. **1986**, *16*, 74-78.

12. Argiz, C.; Sanjuán, M.A.; Muñoz-Martialay, R. Effect of the aggregate grading on the concrete air permeability. *Mater Constr.* **2014**, *64*, e026.
13. Hansen, A.J.; Ottosen, N.S.; Petersen, C.G. Gas-Permeability of Concrete In situ: Theory and Practice. In: Proceedings of ACI SP-82-27: In situ/nondestructive testing of concrete. Detroit, Michigan, USA, 1984, 543-556.
14. Cabrera, J.G.; Lynsdale, C.J. A new gas permeameter for measuring the permeability of mortar and concrete. *Mag Concr Res.* **1988**, *40*, 177-182.
15. Zhang, P.; Li, Q. Effect of polypropylene fiber on durability of concrete composite containing fly ash and silica fume. *Composites: Part B.* **2013**, *45*, 1587-1594.
16. Mills, R.H. Mass transfer of water vapour through concrete. *Cem Concr Res.* **1985**, *15*, 74-82.
17. Tanahashi, I. Evaluation of Durability for Concrete in Terms of Watertightness by Permeability Coefficient Test Results. In: Proceedings of ACI SP-100-13: Concrete Durability. Detroit, Michigan, USA, 1987.187-206.
18. Khoury, G.A. Effect of fire on concrete and concrete structures. *Prog Struct Eng Mat.* **2000**, *2*, 429-447.
19. Box, G.E.P.; Hunter, J.S.; Hunter, W.G. Statistics for Experimenters: Design, Innovation, and Discovery. John Wiley&Sons, New York, USA, 2005.
20. Sanjuán, M.A.; Argiz, C. The new European standard on specifications for common cements UNE-EN 197-1:2011. *Mater Constr.* **2011**, *62*, 425-430.
21. RILEM TC 116-PCD. Permeability of concrete as a criterion of its durability Final report: Concrete durability - An approach towards performance testing. *Mater Struct.* **1999**, *32*, 163-173.
22. Lafhaj, Z.; Richard, G.; Kaczmarek, M.; Skoczylas F. Experimental determination of intrinsic permeability of limestone and concrete: Comparison between in situ and laboratory results. *Build Environ.* **2007**, *42*, 3042-3050.
23. Armstrong, R.A.; Slade, S.V.; Eperjesi, F. An introduction to analysis of variance (ANOVA) with special reference to data from clinical experiments in optometry. *Ophthalmic Physiol Opt.* **2000**, *20*, 235-241.